Molecules and Cells

OPTHiS Identifies the Molecular Basis of the Direct Interaction between CSL and SMRT Corepressor

Gwang Sik Kim[1], Hee-Sae Park[1], and Young Chul Lee[1,*]

[1]School of Biological Sciences and Technology, Chonnam National University, Gwangju 61186, Korea
*Correspondence: yclee@jnu.ac.kr
http://dx.doi.org/10.14348/molcells.2018.0196
www.molcells.org

Notch signaling is an evolutionarily conserved pathway and involves in the regulation of various cellular and developmental processes. Ligand binding releases the intracellular domain of Notch receptor (NICD), which interacts with DNA-bound CSL [CBF1/Su(H)/Lag-1] to activate transcription of target genes. In the absence of NICD binding, CSL down-regulates target gene expression through the recruitment of various corepressor proteins including SMRT/NCoR (silencing mediator of retinoid and thyroid receptors/nuclear receptor corepressor), SHARP (SMRT/HDAC1-associated repressor protein), and KyoT2. Structural and functional studies revealed the molecular basis of these interactions, in which NICD coactivator and corepressor proteins competitively bind to β-trefoil domain (BTD) of CSL using a conserved φWφP motif (φ denotes any hydrophobic residues). To date, there are conflicting ideas regarding the molecular mechanism of SMRT-mediated repression of CSL as to whether CSL-SMRT interaction is direct or indirect (via the bridge factor SHARP). To solve this issue, we mapped the CSL-binding region of SMRT and employed a 'one- plus two-hybrid system' to obtain CSL interaction-defective mutants for this region. We identified the CSL-interaction module of SMRT (CIMS; amino acid 1816-1846) as the molecular determinant of its direct interaction with CSL. Notably, CIMS contains a canonical φWφP sequence (AP*WRP*, amino acids 1832-1837) and directly interacts with CSL-BTD in a mode similar to other BTD-binding corepressors. Finally, we showed that CSL-interaction motif, rather than SHARP-interaction motif, of SMRT is involved in transcriptional repression of NICD in a cell-based assay. These results strongly suggest that SMRT participates in CSL-mediated repression via direct binding to CSL.

Keywords: CSL, Notch, OPTHiS, SMRT, φWφP motif

INTRODUCTION

Notch signaling is an evolutionary conserved pathway that plays a pivotal role in the regulation of various cellular and developmental processes (Borggrefe and Oswald, 2009; Kumar et al., 2017). Upon ligand binding through the cell-to-cell contact, the intracellular domain of Notch receptor (NICD) is released by proteolytic cleavage and activates transcription of target genes via the direct interaction with the DNA-bound transcription factor CSL (for vertebrate CBF1/RBP-J, *Drosophila* Suppressor of Hairless, and *C. elegans* Lag-1) (Borggrefe and Oswald, 2009; Kopan and Ilagan, 2009). The structural study revealed that a core region of CSL is consisted of three distinct domains; N-terminal (NTD), β-trefoil (BTD), and C-terminal (CTD) domains (Kovall and Hendrickson, 2004). The association of NICD with CSL creates a coactivator-binding surface that is recognized by the essential coactivator Mastermind (MAM). Subsequent structural studies showed that two fundamental molecular

Received 4 May, 2018; revised 18 June, 2018; accepted 19 July, 2018; published online 30 August, 2018

eISSN: 0219-1032

interactions are essential for the formation of CSL/NICD/MAM complex (Nam et al., 2006; Wilson and Kovall, 2006). First, the RAM (RBP-J-associated molecule) domain of NICD interacts with the CSL-BTD with high affinity. A φWφP motif (φ denotes any hydrophobic residues), which is highly conserved in the RAM domains of all Notch proteins, is identified to be essential for CSL interaction. Second, low affinity-binding of ankyrin repeats of NICD with CSL-CTD generates the binding interface for MAM coactivator, in which the helical domain of MAM binds to a continuous groove formed by the CTD-ankyrin interface and the β-sheet of NTD (Kovall and Blacklow, 2010). The CSL/NICD/MAM coactivator complex can subsequently recruit the secondary coactivators such as histone acetyltransferase p300 to achieve the transcriptional activation (Oswald et al., 2001).

In the absence of NICD binding, DNA-bound CSL recruits various corepressor proteins to down-regulate target gene expression. Therefore, CSL-mediated repression *vs.* activation represents the coregulator exchange mechanism, in which NICD binding displaces corepressors from CSL and provides a novel interface for coactivator MAM recruitment. To date, the list of CSL-interacting corepressors includes SMRT/NCoR (silencing mediator of retinoid and thyroid receptors/nuclear receptor corepressor), SHARP/MINT (SMRT/HDAC1-associated repressor protein/*MSX2*-interacting nuclear target protein), *Drosophila* Hairless, CIR (CBF1-interacting corepressor), KyoT2, and RITA (RBP-J-interacting tubulin-associated) (Borggrefe and Oswald, 2009; Collins et al., 2014; Hsieh et al., 1999; Kao et al., 1998; Oswald et al., 2002; Wacker et al., 2011). The structural studies regarding CSL-corepressor interactions have been extensively pursued. Crystal structures of the CSL-KyoT2 and CSL-RITA corepressor complexes demonstrate that these corepressors associate with CSL-BTD with a mode similar to that of NICD-binding to BTD (Collins et al., 2014; Tabaja et al., 2017). A φWφP sequence, which is known as BTD-binding motif of RAM domains, is also identified as the molecular determinants of the interactions of KyoT2 and RITA with CSL-BTD. These results provide the molecular basis of coregulator exchange via the competitive binding of corepressor (KyoT2 and RITA) *vs.* coactivator (NICD-RAM) to a common target (CSL-BTD). However, detailed structural data indicates that the binding interfaces of CSL-BTD with these interactors are not identical. Recently, Yuan et al. unveil the structural and molecular details of Suppressor of Hairless [Su(H); CSL ortholog in flies] in complex with the corepressor Hairless, which is the major antagonist of Notch signaling in *Drosophila* (Yuan et al., 2016). Intriguingly, Hairless exclusively interacts with the hydrophobic core of the Su(H)-CTD, which results in a dramatic conformational changes within CSL-CTD. This structural plasticity blocks the CTD-NICD interaction and explains the molecular basis of mutually exclusive bindings of NICD and Hairless to Su(H)-CTD.

SMRT and NCoR are ubiquitously expressed corepressor proteins containing three autonomous repression domains in their N-terminal regions (Chen and Evans, 1995; Mottis et al., 2013). Each of the repression domains plays a non-redundant role in the platform for recruitment of various DNA-binding repressors or corepressors, including MyoD, Bcl6, and histone deacetylases (Huang et al., 2000). *In vivo*, SMRT/NCoR exists in a steady-state complex containing HDAC3, which has been implicated in Notch signaling (Oberoi et al., 2011; Pajerowski et al., 2009). A pioneer work by Kao et al. showed that CSL factor is a direct interaction partner of SMRT/NCoR corepressors (Kao et al., 1998). A novel CSL-interacting domain of SMRT (amino acids 1679-1841 of full-length SMRT) has been mapped for the direct interaction with CSL both *in vitro* and *in vivo*. Interestingly, this domain could not bind a CSL-BTD mutant (EEF233AAA) that is defective in repressive function, suggesting that SMRT is a bona fide and physiological corepressor of CSL. SHARP (also known as MINT in mouse) protein was also identified as a corepressor for CSL-mediated transcriptional regulation (Oswald et al., 2002; VanderWielen et al., 2011). SHARP interacts with both the BTD and CTD of CSL and interactions of SHARP or NICD with CSL are mutually exclusive. Interestingly, SHARP is thought to be a Hairless counterpart in mammals, raises the possibility that SHARP binds the CSL-CTD as in the case of Hairless binding to Su(H)-CTD (Yuan et al., 2016). In particular, SHARP has a conserved C-terminal SPOC domain that is essential for corepressor function via the direct interaction with conserved acidic motif at the C-terminal region of SMRT/NCoR (Ariyoshi and Schwabe, 2003; Mikami et al., 2014). Based on this finding, SHARP is suggested as the bridge factor between CSL and the SMRT corepressor.

In this report, we tried to address the molecular basis for the direct interaction between CSL and SMRT. Our results suggested that CIMS can directly interact with CSL-BTD using canonical φWφP sequence (AP*IWRP*, amino acids 1832-1837), in a manner similar to other BTD-binding corepressors (KyoT2 and RITA), without the aid of bridge factor like SHARP.

MATERIALS AND METHODS

Plasmids

Details of pCMV-flag-CSL (amino acids 21-500 of hCSL), pGEX-4T-SD2 (amino acids 1594-2104 of hSMRT), and 4XCBS luciferase reporter were described previously (Ann et al., 2012). To construct pRS325LexA-CSL and -CIMS (amino acids 1816-1846 of hSMRT), the corresponding DNAs were amplified by PCR and inserted into the *Bam*HI/*Xho*I sites of pRS325LexA. pB42AD-SD2 was constructed by PCR amplification of insert and cloning into the *Eco*RI/*Xho*I sites of pB42AD. For OPTHiS (one- plus two-hybrid system) screening, SD2b (amino acids 1750-1952) and CIMS regions were amplified by PCR and inserted into the *Eco*RI/*Bam*HI sites of pRS324UBG vector. For bimolecular fluorescence complementation (BiFC) assay, KGN-MC-SD2b and -CIMS were constructed by subcloning the *Kpn*I/*Xho*I fragment of pcDNA3-HA-SD2b or -CIMS into the same sites of KGN-MC vector (MLB International Corporation). KGC-MC-CSL was made by PCR amplification of CSL and subcloning into the *Kpn*I/*Xho*I sites of KGC-MC vector. For GST pull-down assay, CSL-interaction defective (CID) mutants of CIMS were obtained from the pRS324UBG constructs and subcloned into pGEX4T-1 using enzyme sites. To introduce single-point

mutations into the pB42AD-SD2 (W1835R and P1837S), KGN-MC-SD2b (I1834S and R1836G), pcDNA3-HA-CSL (F235R, V237R, A245R, and Q307R), or pCMX-mSMRT-flag (W1793R and/or W2383stop), the site-directed mutagenesis was performed using Quickchange II site-directed mutagenesis kit according to the manufacturer's instruction (Agilent technologies). KGN-MC-SD2b mutants (A1832V, W1835R, and P1837S) and pGEX4T-SD2 mutants (W1835R and P1837S) were derived from pRS324UBG and pB42AD constructs, respectively. To make pLGZ-4XCBS *LacZ* reporter plasmid, the DNA fragment containing four repeats of the CBS (CSL-binding site) was obtained from the 4XCBS luciferase reporter by PCR and inserted into the *Xho*I site of the pLGZ vector. pRS325GU-CSL was made by subcloning of *Bam*HI/*Xho*I fragment from KGC-MC-CSL into the same sites of pRS325GU. To construct pGEX4T-RAM and KGN-MC-LAM-LC constructs, RAM (amino acids 322-441) or RANM-LC (amino acids 367-441) from mouse Notch1 was amplified by PCR and inserted into the *Eco*RI/*Xho*I sites of the pGEX4T-1 and the *Kpn*I/*Xho*I sites of the KGN-MC vector, respectively. pGEX4T-CIMK was prepared by PCR-amplification of CIMK (CSL-interaction module of KyoT2; amino acids 172-202) region (amino acids 172-202) of KyoT2 and subcloning into the *Eco*RI/*Xho*I sites of the pGEX4T-1. All constructs were confirmed by DNA sequencing.

Mutagenic PCR and OPTHiS screening

Random mutagenesis and OPTHiS screening of SD2b and CIMS fragments were conducted as previously described (Kim et al., 2012). Briefly, mutagenic PCR fragment containing the SD2b or CIMS region was amplified using pRS324UBG-SD2b or -CIMS as PCR templates, respectively. Mutagenic PCR products (2 μg) were co-transformed with the linearized gap plasmids (400 ng) into yeast strain YOK400 (*MATa, leu2, trp3, ura3, lexA$_{op}$-LEU2, UAS$_{GAL}$-HIS3*) carrying the pSH18-34 reporter (8X*lexA$_{op}$-LacZ*) as well as the bait plasmid pRS325LexA-CSL. For the actual screening, a large number of transformants was obtained from several batches of standard-scale transformation. After 3 days of incubation at 30°C on synthetic glucose media lacking histidine, 2,000-3,000 transformants were picked on X-gal plates to test the two-hybrid interaction. White colonies were selected as CID mutants and subsequent verification was carried out as described (Kim et al., 2012).

Cell culture and transient transfection assay

HEK293 cells were maintained in DMEM (Welgene) supplemented with 10% fetal bovine serum (Welgene) and antibiotics-antimyces (Gibco). Cells were seeded in 24-well plates with 5-8 X 10^4 cells/well on the day prior to transfection. Transient transfections were performed using the TurboFect (Fermentas) systems. After 48 h of transfection, whole-cell lysates were prepared with RIPA buffer [50 mM Tris-HCl (pH 8.0), 5 mM EDTA, 150 mM NaCl, 1% NP-40, 1 mM PMSF] and used for luciferase and β-galactosidase activity for each sample.

BiFC assay and confocal laser-scanning microscopy

Bimolecular fluorescence complementation (BiFC) assays were carried out using a Fluo-Chase kit (Amalgaam). SMRT fragments (SD2b or CIMS) and CSL derivatives were fused to the N- and C-terminal portions of Kusabira Green protein, respectively, resulting in KGN-SD2b/CIMS and KGC-CSL constructs. After 48 h of transfection of these constructs in HEK293, the fluorescent signals (excitation wavelength: 494 nm, emission wavelength: 538 nm) from the prepared whole-cell lysates were measured using a fluorescence spectrometer (Molecular Devices, Spectra max GEMINIXPS). For confocal laser scanning microscopy, HEK293 cells were grown on 8-well slide plates (SPL Life science) and co-transfected with KGN-SD2b and KGC-CSL constructs. After 48 h of transfection, cells were fixed in 4% paraformaldehyde for 10 m at room temperature, mounted onto micro cover-slides, and observed for green fluorescence using a laser-scanning confocal microscope (Leica TCS SPE).

Yeast interaction assay and GST pull-down assay

Yeast strain EGY48 containing pSH18-34 was co-transformed with the expression plasmids for LexA-fused bait and B42AD-/B42-GBD-fused prey by the lithium acetate method. In a natural promoter reporter assay, EGY48 containing pLGZ-4XCBS reporter plasmid (instead of pSH18-34) was co-transformed with pRS325GU-CSL and pRS324UBG-CIMS mutants. Liquid assays for β-galactosidase activity were carried out as described (Kim et al., 2007).

For GST pull-down assay, Flag-tagged CSL proteins were labeled with ^{35}S-methionine using a TNT *in vitro* translation kit (Promega). The radiolabeled proteins were mixed with equivalent amounts of GST or GST-fused proteins bound to glutathione-agarose beads (Sigma-Aldrich) pre-equilibrated with GST binding buffer. The beads were washed and the bound proteins were analyzed by 8% SDS-PAGE followed by autoradiography. Details of the preparation of GST proteins and pull-down condition were described in previous report (Kim et al., 2012).

Statistical analysis

All quantitation experiments were repeated two or three times for the triplicated samples. The student's *t*-test was used to measure statistically significant differences between control (wild-type) and sample (mutant) groups in the corresponding graphs and their *p*-values were less than 0.005 in all cases except for Fig. 5B.

RESULTS AND DISCUSSION

Mapping of CSL-binding domain within SMRT corepressor

As we mentioned, it was reported that CSL interacts with specific region of SMRT (amino acids 1679-1841 of full-length hSMRT) in the yeast-two hybrid and GST pull-down assays (Kao et al., 1998). We chose SD2 region of hSMRT (amino acids 1594-2104) and tested its interaction with CSL in the yeast two-hybrid assay, resulting in observation of the strong binding between them (Supplementary Fig. S1B). To minimize the SMRT region for CSL binding, we further divided SD2 domain into three overlapping parts (Supplementary Fig. S1A) and tested their abilities to interact with CSL in the yeast-two hybrid and GST pull-down assays. Only SD2b

(amino acids 1750-1952) domain interacts with CSL in these assay systems (Supplementary Figs. S1B and S1C). Notably, SD2b region is nicely overlapped with the SMRT region (amino acids 1679-1841) previously mapped by Kao et al. (1998) for CSL binding.

Isolation of the CSL interaction-defective (CID) alleles of SD2b region by OPTHiS

In order to understand the molecular basis of the interaction between CSL and SD2b of the SMRT, we employed OPTHiS (one- plus two-hybrid system) to determine the amino acid residues of SD2b essential for CSL binding. OPTHiS is the modified version of the conventional yeast two-hybrid system for the efficient selection of the missense mutant alleles that specifically disrupt a known protein-protein interaction (Kim et al., 2012). As a first step to isolate the full-length missense alleles of SD2b, mutagenic PCR fragment of SD2b was co-transformed into the yeast strain YOK400 with the linearized gap plasmid (Fig. 1A) as described in "Materials and Methods". During yeast transformation, a gap repair process was occurred at the linearized gap plasmids using SD2b fragments as templates, resulting in the one-step construction of mutant cell library for SD2b region. The transformants were grown in synthetic glucose medium lacking histidine for the positive selection of intact prey fusion (B42-SD2b-GBD) using the endogenous UAS$_{GAL}$-*HIS3* reporter gene. For the second step of screening of the non-interactor, we picked about 2,000 transformants on X-gal plate and a total of 6 white colonies were finally obtained as candidates of CID mutants of SD2b after verification. Surprisingly, all the isolated CID alleles of SD2b are located only in adjacent three residues of SD2b (A1832, W1835, and P1837) as mutational hotspots (Fig. 1B) and these SD2b mutants were not able to interact with CSL in the liquid β-galactosidase assay (Fig. 1C). This information revealed the novel findings that a short motif (1832 APIWRP 1837) within the SD2b region is directly involved in CSL interaction and this motif contains a φWφP sequence conserved in all BTD-binders (Figs. 1B and 6A).

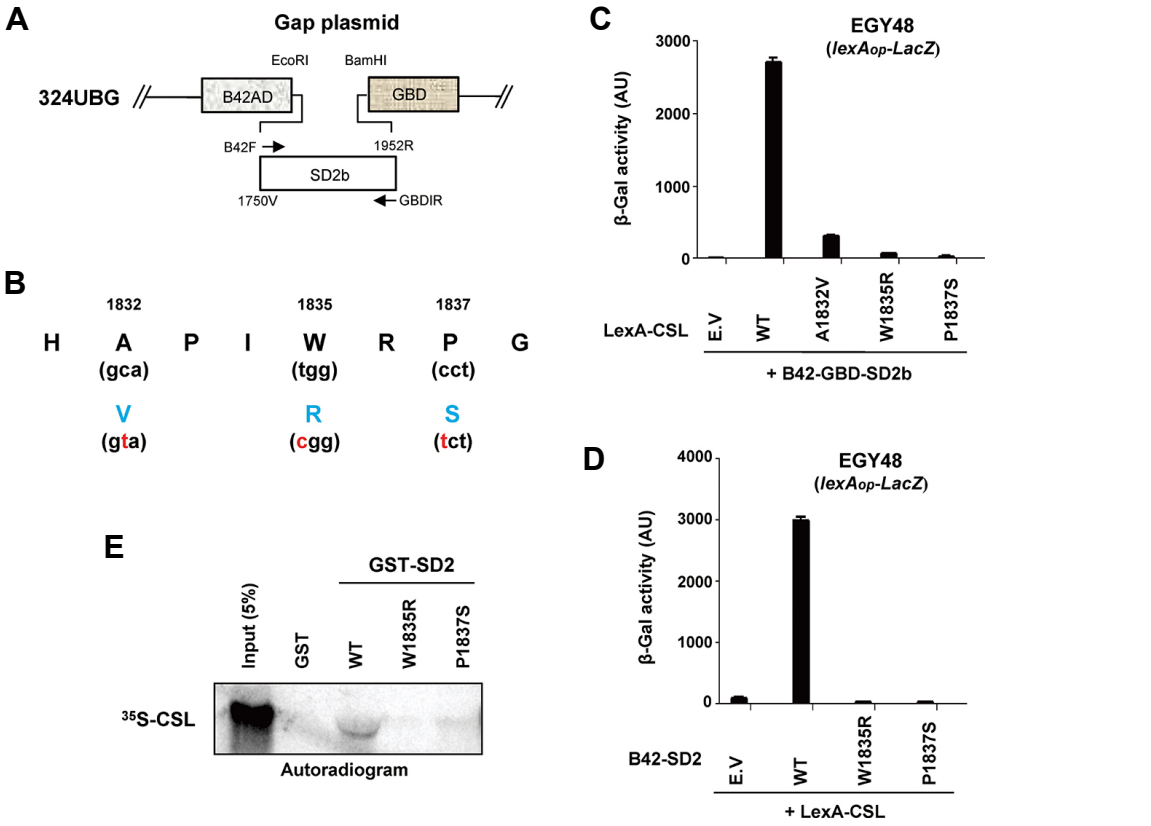

Fig. 1. CSL interaction-defective (CID) mutants of SD2b obtained by OPTHiS. (A) Schematic depiction of gap plasmid and SD2b region of SMRT used for CID mutant screening by OPTHiS. (B) The position and residues of the isolated CID mutants of SD2b. The blue and red letters indicate the changed amino acids and nucleotides, respectively. (C) Defective interactions between SD2b mutants and CSL in the yeast two-hybrid assay. The plasmid expressing the LexA-CSL was co-transformed into EGY48 with the B42-GBD prey plasmids expressing SD2b mutants or B42AD-GBD alone. Liquid β-galactosidase assays were carried out as described and the mean ± SE values are shown on the y-axis. E.V, empty vector. (D, E) Defective interactions of CSL with the CID mutants of SD2 context. (D) Yeast-two hybrid assay. The yeast strain EGY48 was expressed with LexA-CSL and the B42-fused SD2 mutants or B42AD alone. E.V, empty vector. (E) GST pull-down assay. *In vitro* translated and ^{35}S-labeled CSL were incubated with the indicated GST-fused proteins of SD2 derivatives and the bound proteins were analyzed as described.

To verify the relevance of this interaction, we attempted to examine the mutational effect of these residues on the interaction between CSL and SD2 region (~500 amino acids). We introduced W1835R or P1837S mutation into SD2 region and tested for their interactions with CSL in the yeast two-hybrid and GST pull-down assays (Figs. 1D and 1E). Consistent with SD2b mutant data, the same mutations in SD2 context abolished CSL-SD2 interactions, confirming the importance of a φWφP sequence of SMRT in CSL binding. We also made a full-length SMRT mutant having each of these mutations and investigated their CSL-binding activities in GST pull-down assay. Unfortunately, we could not obtain positive result due to the low expression level of full-length SMRT protein and its sticky property (data not shown).

CIMS region of SMRT is sufficient for CSL interaction

Based on SD2b mutant data, we tried to minimize SD2b region essential for CSL binding and designed a CSL-interaction module of SMRT (CIMS, amino acids V1816 to S1846), which contains the core φWφP motif (1832 APIWRP 1837) in a middle (Fig. 2A). In the yeast two-hybrid assay, CIMS fused between B42 and GBD was able to interact well with LexA-CSL although their binding strength is approximately one third of that of CSL-SD2b interaction (Fig. 2B). Next, we employed the bimolecular fluorescence complementation (BiFC) assay to demonstrate the interaction between CIMS and CSL in mammalian cells. BiFC assay is a novel assay method for the protein-protein interactions occurred in living cells and is independent of transcription system. First, we constructed the expression plasmids for the N-terminal portion of the Kusabira Green protein (KGN) fused with SD2b or CIMS as well as the C-terminal portion of this protein (KGC) fused with CSL. If SD2b or CIMS can interact with CSL, a green fluorescence signal would be generated from the reconstituted Kusabira Green protein. After 48 h of transfection of these plasmids into HEK293 cells, a fluorescence signal from the prepared whole-cell extracts was measured using a fluorescence spectrometer. As shown in Fig. 2C, the association of KGC-CSL with KGN-SD2b increased the fluorescence signal two-fold above the background signal generated by KGN empty vector. Consistent with the yeast two-hybrid data, KGN-CIMS can interact with KGC-CSL with a lower affinity than that of SD2b (Fig. 2C). When BiFC assays were performed with the intact cells using a confocal microscope, we observed that the numbers of cells expressing a fluorescence signal were in a good agreement with the quantitative data (Figs. 2C and 2D). Taken together, CIMS is sufficient for CSL interaction in yeast and mammalian cells, demonstrating that the core φWφP motif (APIWRP, amino acids 1832-1837) is solely responsible for SD2 binding to CSL. However, as mentioned, the affinity of CIMS-CSL binding is relatively weaker than that of SD2b-CSL binding. We assumed that the additional regions in SD2b might have a stabilizing effect on CIMS-CSL interaction, which plays a significant role in the high-affinity binding between SMRT and CSL *in vivo*.

Isolation of CID mutant alleles for CIMS region by OPTHiS

To obtain more detailed information about the binding interface between SMRT and CSL, we performed the second round of OPTHiS screening for the isolation of CID mutants using CIMS as a target region. Basically, the OPTHiS procedure to isolate CIMS CID mutants is identical to that of previous screening for SD2b mutants. However, considering the size of CISM (31 amino acids), we expect that this would be an intensive mutant screening through the saturated mutagenesis. The mutagenic PCR products of CIMS and the linearized gap plasmids were prepared (Fig. 3A) and co-transformed into the YOK400 strain expressing LexA-CSL.

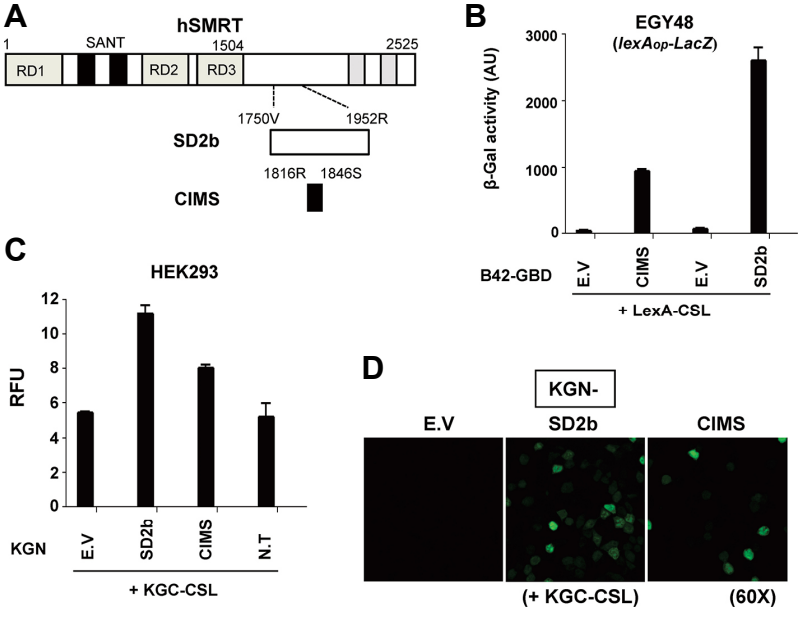

Fig. 2. The CIMS region of SMRT is sufficient for CSL interaction. (A) Schematic diagram of SD2b and CIMS regions. (B-D) The CIMS region is sufficient for CSL interaction. (B) Yeast two-hybrid assay. EGY48 was co-transformed with LexA-CSL construct and the prey plasmids expressing B42AD-GBD-fused CIMS or SD2b. E.V, empty vector. (C) Quantitative BiFC assay. The expression vectors the KGN-SD2b or -CIMS and the KGC-CSL were transiently transfected into HEK293 cells. After 48 h of transfection, the fluorescent signals from the prepared whole-cell extracts were measured using fluorescence spectrophotometer. E.V (empty vector) and N.T (no transfection) were used as negative controls. RFU, relative fluorescence units. (D) Confocal laser-scanning microscopic images from the intact cells in BiFC assay (C). *Magnification*: 60X.

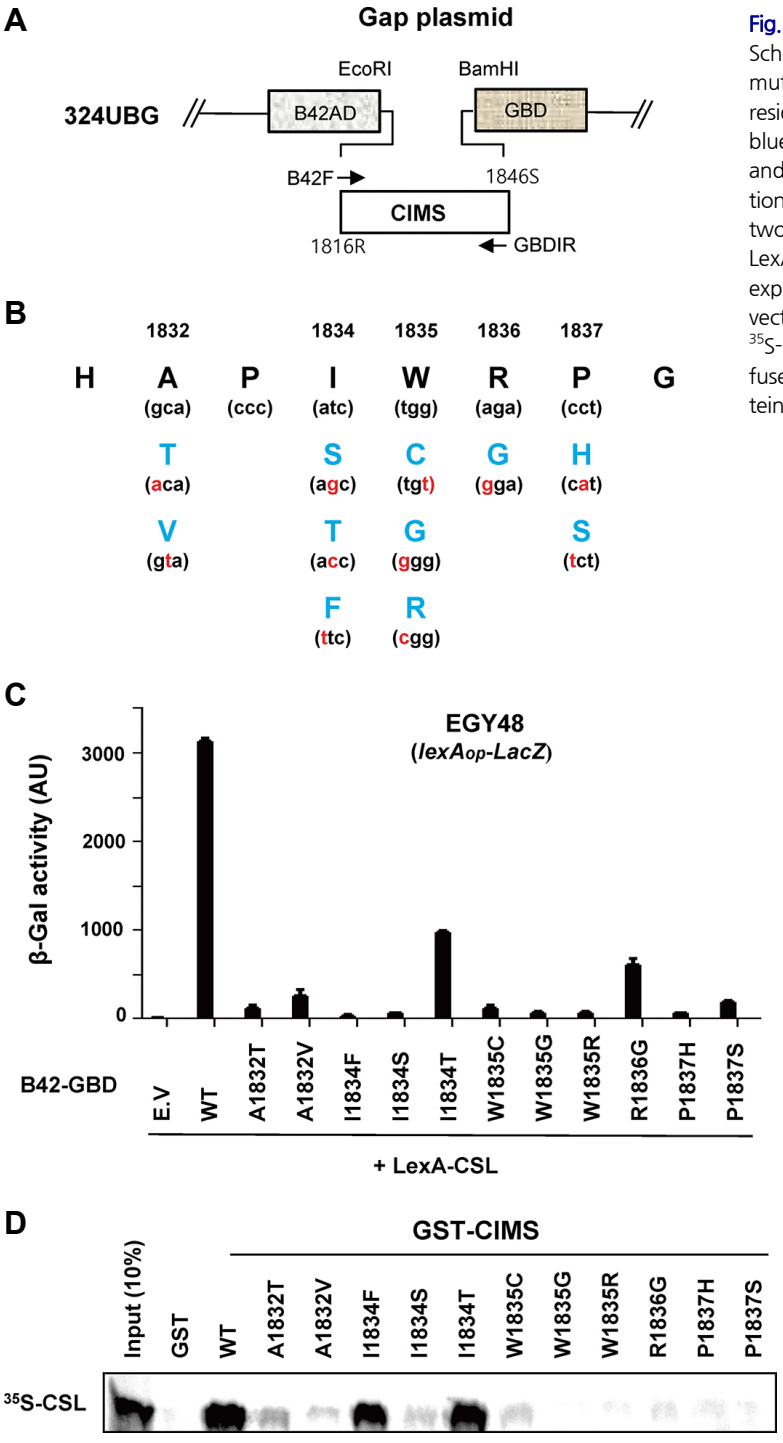

Fig. 3. CID mutants of CIMS obtained by OPTHiS. (A) Schematic diagram of gap plasmid and CIMS region for mutant screening by OPTHiS. (B) The positions and residues of the isolated CID mutants by OPTHiS. The blue and red letters indicate the changed amino acids and nucleotides, respectively. (C, D) Defective interactions of CSL with the CID mutants of CIMS. (C) Yeast-two hybrid assay. EGY48 was co-transformed with the LexA-CSL bait plasmid and the indicated prey plasmids expressing B42-GBD-fused CIMS mutants. E.V, empty vector. (D) GST pull-down assay. *In vitro* translated and ^{35}S-labeled CSL were incubated with the indicated GST-fused proteins of CIMS mutants and the bound proteins were analyzed.

After non-interactor screening of 3,000 transformants on X-gal plates, a total of 11 CID mutant alleles were finally isolated. Figure 3B shows the mutational sites found in the isolated CIMS mutants with the nucleotide and amino acids changes. Compared to SD2b mutant alleles, more than one mutations were found at A1832 (to T, V), W1835 (to C, G, R), and P1837 (to H, S) residues as hotspots, indicating the intensiveness of this mutant screening. Notably, we could find new mutations at two additional residues within CIMS, I1834 (to S, T, F) and R1836 (to G), which corresponds to hydrophobic residues within the core φWφP motif (IWRP). These results indicated that the CSL-binding motif of CIMS is defined as APIWRP, in which A1832 and φWφP sequence have critical roles in CSL binding.

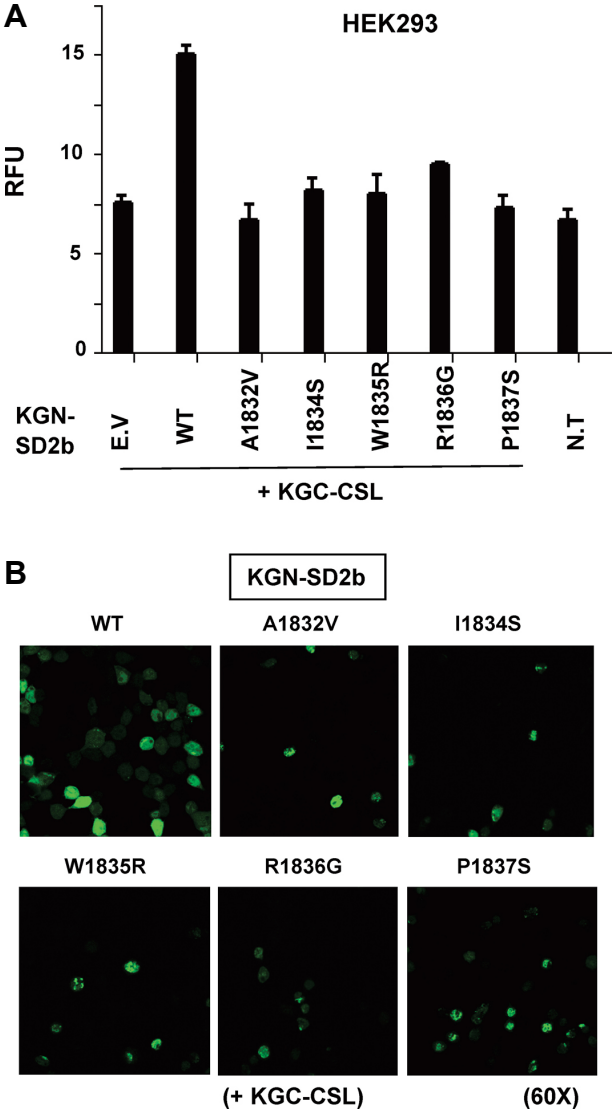

Fig. 4. Defective interactions of CIMS mutants with CSL in mammalian cells. (A) Quantitative BiFC assay. The expression vectors the indicated KGN-SD2b mutants and the KGC-CSL were transiently transfected into HEK293 cells. After 48 h of transfection, the fluorescent signals from the whole-cell extracts were measured. E.V, empty vector; N.T, no transfection; RFU, relative fluorescence units. (B) Confocal laser-scanning microscopic images from the intact cells in BiFC assay (A). *Magnification*: 60X.

As a next step, we demonstrated the defective interactions of CIMS mutants with CSL in the yeast two-hybrid and GST pull-down assays (Figs. 3C and 3D). In a liquid β-galactosidase assay, all CIMS mutants showed complete defects in CSL binding in yeast even though two mutants (I1834T and R1836G) have weak binding activity (Fig. 3C). To confirm these results *in vitro*, we performed GST pull-down assay using *in vitro* translated [^{35}S]-labeled CSL and bacterially expressed GST-fused CIMS mutants (Fig. 3D). We observed that nine CIMS mutants had negligible binding activities to CSL when compared to that of wild-type CIMS. However, inconsistent with the yeast two-hybrid data, two mutants (I1834F, I1834T) showed no significant defects in CIMS-CSL interaction. This allele-specific effect suggests that I1834 residue would be directly involved in the interaction with CSL. Next, we evaluate these interactions in mammalian cells via BiFC experiments (Fig. 4). Because BiFC signals generated by the association of KGN-CIMS and KGC-CSL was too weak to quantitatively analyze (Figs. 2C), we selected five CIMS mutations (A1832V, I1834S, W1835R, R1836G, and P1837S) and introduced them into SD2b region. When KGN-SD2b mutants were tested for their association with KGC-CSL in quantitative BiFC assay, all of these mutants were not able to interact with CSL (Fig. 4A). This result was consistently reproduced in BiFC image analysis using intact cells, in which the number of the HEK293 cells expressing a fluorescence signal were significantly decreased in the samples transfected with KGN-SD2b mutants when compared to that of the wild-type SD2b (Fig. 4B). Overall, these results indicate that the CSL-binding motif of SMRT (APIWRP) identified by OPTHiS is actually responsible for CSL binding *in vivo* as well as *in vitro*.

Defective interactions of CIMS mutants with native form of CSL in yeast natural promoter assay

There are many convincing evidences for the molecular switch of CSL from a repressor to an activator through the competitive bindings of corepressor and coactivator to CSL-BTD (Borggrefe and Oswald, 2016). If SMRT participates in the transcriptional repression of CSL-bound target genes via direct interaction, it is plausible that CID mutations obtained by OPTHiS also abolish CIMS interaction with a native form of CSL in yeast natural promoter assay. Actually, the hybrid forms of CSL (fused with LexA or KGC) were used in all cases of OPTHiS screening and evaluations of CSL-binding activities of CIMS mutants. To address this issue, we made the CSL-driven *LacZ* reporter plasmid (pLGZ-4XCBS), which contains four copies of CBS (5′-CGTGGGAA-3′), and the bait plasmid expressing a native form of CSL (pRS325GU-CSL) (Fig. 5A). After pRS324UBG-CIMS wild-type or CID mutants were transformed into EGY48 strain harboring pLGZ-4XCBS and pRS325GU-CSL, each of the transformation samples was tested for CSL-CIMS interactions in a liquid β-galactosidase assay. As shown in Fig. 5B, all of CIMS mutants lost their binding abilities to a native form of CSL bound at CBS of reporter gene. These results demonstrated that CSL-binding motif of CIMS obtained by OPTHiS is also involved in the interaction with native form of CSL and probably in the SMRT-mediated repression of Notch target genes.

CIMS binds to CSL-BTD using conserved φWφP motif

Because CSL-binding motif of CIMS contains a φWφP sequence, we expect that CIMS interacts with BTD region of CSL as other BTD-binders harboring a φWφP motif. To confirm this interaction, we divided full-length CSL into three sub-domains containing NTD (CSLa, amino acids 21-260), BTD (CSLb, amino acids 141-380), and CTD (CSLc, amino acids 261-500), respectively (Supplementary Fig. S2A), and

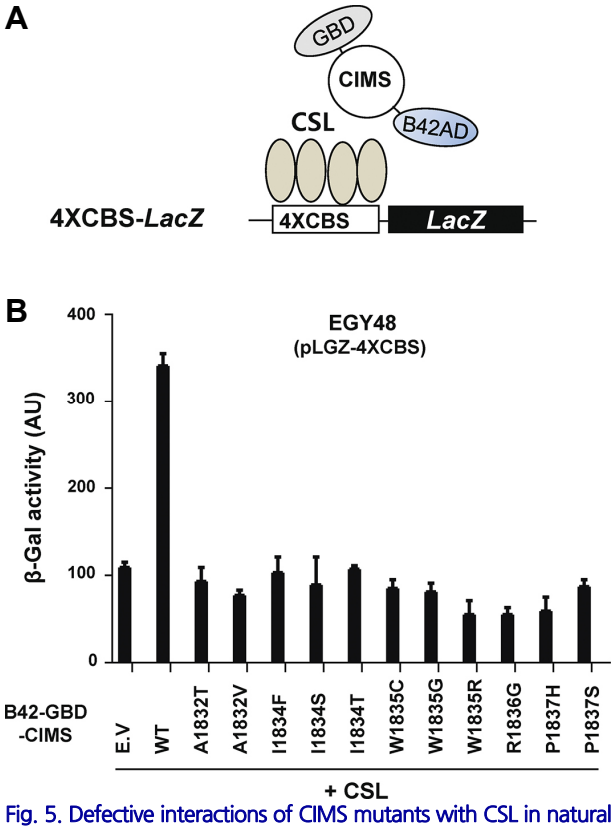

Fig. 5. Defective interactions of CIMS mutants with CSL in natural promoter assay. (A) Schematic depiction of CSL-driven *LacZ* reporter, 4XCBS-*LacZ*. The CIMS region fused between B42AD-GBD interacts with native form of CSL formed on natural promoter containing four-copies of CBS. (B) Yeast two-hybrid assay. The bait plasmid expressing the native form of CSL was introduced into EGY48 strain harboring pLGZ-4XCBS reporter along with the prey vectors expressing the indicated CIMS mutant. The *p*-values obtained by student's *t*-test are less than 0.03 in all compared groups between wild-type and mutants. E.V, empty vector.

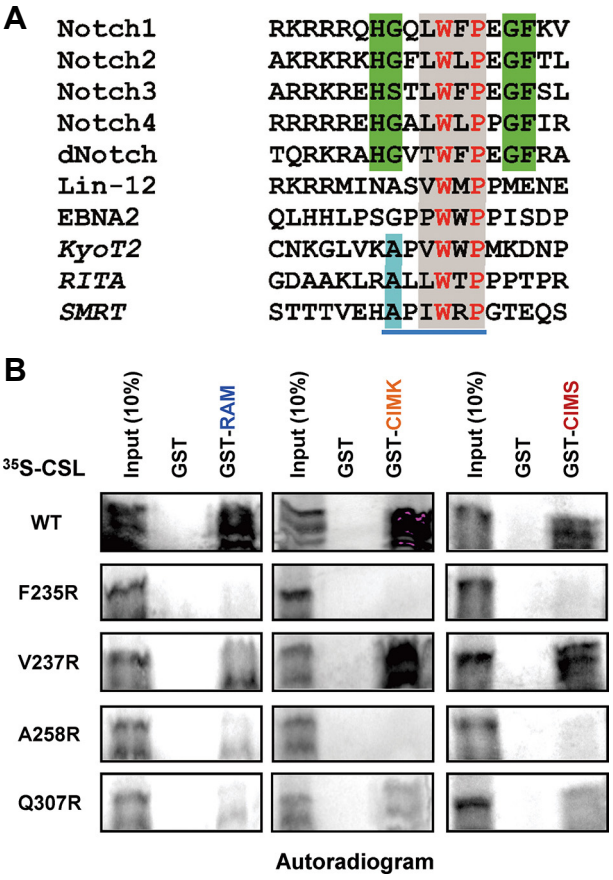

Fig. 6. CIMS interacts with CSL in a manner similar to other corepressors using a conserved φWφP motif. (A) Sequence alignment of the CSL-binding region of CIMS with the corresponding regions of RAM domains of Notch1-4, *Drosophila* Notch (dNotch), *C. elegans* Notch (LIN-12), Epstein-Barr virus nuclear antigen 2 (EBNA2), KyoT2, and RITA proteins. The core motif within CIMS region is underlined with blue color. Grey box, φWφP motif; Green box, basic dipeptide motifs found in Notch proteins; blue box, alanine residue found in corepressors. (B) Interactions of the indicated CSL mutants with CIMS, RAM, and CIMK in GST pull-down assays. Wild-type (WT) or mutants (F235R, V237R, A258R, and Q307R) CSL proteins were labeled with ^{35}S-methionine via *in vitro* translation and incubated with GST alone or GST-fused CIMS, RAM (amino acids 322-441 of mNotch1), or CIMK (amino acids 172-202 of KyoT2) proteins. The bound proteins were analyzed by SDS-PAGE and autoradiography.

investigated their interactions with CIMS in the yeast two-hybrid assay. In a liquid β-galactosidase activity, only CSLb fragment containing BTD strongly interacts with CIMS (Supplementary Fig. S2B), confirming that CIMS bind to the CSL-BTD using a φWφP motif in a manner similar to other proteins having this motif.

We conducted multiple-sequence alignment of the CSL-binding region of CIMS with the corresponding regions of RAM domains of Notch1-4, dNotch, LIN-12, EBNA2, KyoT2, and RITA (Fig. 6A). There is an overall structural similarity in the mode of interactions between these CSL-regulators and CSL-BTD, in which their φWφP motifs exclusively bind a non-polar pocket on the surface of the BTD (Tabaja et al., 2017). However, residues proximal to the φWφP motif are not conserved between coactivators and corepressors and play a different role for CSL binding. For example, it was reported that RAM has additional basic dipeptide motifs (HG and GF) outside of the φWφP that make significant contributions to the high-affinity CSL-RAM binding (Johnson et al., 2010) (Fig. 6A). KyoT2 and RITA lack these additional basic motifs, implying that corepressors and NICD coactivators utilize different binding modes to achieve high-affinity binding to CSL. In this regard, V186 residue of KyoT2 (VKAP*VWWP*) is shown to make extensive hydrophobic contacts with F222 and V224 residues of CSL to achieve the high-affinity KyoT2-CSL binding (Collins et al., 2014). In CIMS, however, E1830 residue is located in the corresponding position (EHAPIWRP) and this residue is not expected to make hydrophobic inter-

actions with nonpolar residues of the CSL-BTD. Our OPTHiS screening showed that A1832 residue of CIMS (AP*IWRP*) is essential for CSL binding rather than E1830 residue (Fig. 3). The Ala residue in this position is conserved in all the CSL-binding motifs of corepressors (Fig. 6A), suggesting an important role in CSL-BTD binding. In the structures of CSL-corepressor complexes, this Ala residue locates in a hollow groove of non-polar pocket, which is comprised of E233, F235, and A258 residues of CSL (Collins et al., 2014; Tabaja et al., 2017). Based on this, we hypothesized that Thr or Val mutation at A1832 (Fig. 3B) decreases the binding affinity between CIMS and CSL because the bulky side chain of these residues may cause the steric hindrance for CIMS to bind CSL-BTD.

Finally, we searched Swiss-Prot protein database for the core motif sequence found in CSL-binding corepressors using the ScanProsite program and found that the corepressor type of φWφP motif exists only in KyoT2, RITA, and SMRT proteins. Notably, the CSL-interaction motif of SMRT is not conserved in NCoR corepressor, raises the intriguing possibility that the CSL-mediated repression is specifically mediated by SMRT, not by NCoR.

CIMS interacts with CSL in a manner similar to other corepressors

Although the binding modes of corepressors or Notch coactivators to CSL-BTD are generally similar, detailed structural data indicates that the binding interfaces of CSL-BTD with these coregulators are not identical (Borggrefe and Oswald, 2014). In addition, the mutational studies revealed that, among the four CSL-BTD residues critical for RAM binding (F235, V237, A258, and Q307), V235 and Q307 residues are not essential for KyoT2 or RITA binding *in vitro* (Collins et al., 2014; Tabaja et al., 2017). This result is consistent with the notion that residues proximal to the φWφP motif play a different role in CSL binding and there are differential binding modes by corepressors and RAM for CSL. To test the idea that CIMS also utilize the binding mode similar to other corepressor, we constructed four kinds of CSL mutants (F235R, V237R, A258R, and Q307R) and investigated their interactions with CIMS, KyoT2, and RAM domains *in vitro*. First, we measured the binding activities of CSL mutants with CIMS or corresponding regions of KyoT2 (CIMK, CSL-interaction module of KyoT2) or Notch1 (RAM) in the GST pull-down assay (Fig. 6B). In a good agreement with previous *in vitro* data (Collins et al., 2014; Tabaja et al., 2017), all CSL mutants could not interact with NICD-RAM, confirming the importance of these residues in RAM binding. In contrast to this, CIMK was able to interact with V237R and Q307R mutants, but not with F235R and A258R mutants, as expected from the previous results (Fig. 6B). Interestingly, the interaction profile between CSL-BTD mutants and CIMS is similar to that of CIMK (Fig. 6B), demonstrating that the binding mode of CSL-CIMS is a corepressor type of KyoT2 rather than a coactivator type of Notch-RAM.

CSL-interaction motif, rather than SHARP-interaction motif, of SMRT is involved in the transcriptional repression of NICD by SMRT

As mentioned, SHARP/MINT has a conserved C-terminal SPOC domain that is essential for corepressor function via the direct interaction with conserved acidic motif at the C-terminal region of SMRT/NCoR (Ariyoshi and Schwabe, 2003; Mikami et al., 2014). This finding raises the intriguing question that SMRT interacts with CSL directly or indirectly via the bridge factor SHARP. To address this issue, we introduced W1793R or W2383stop mutation into full-length mouse SMRT, which is predicted to abolish its CLS binding (W1793R corresponds to W1835R of hSMRT) or SHARP interaction (W2383stop), respectively. W2383stop mutant

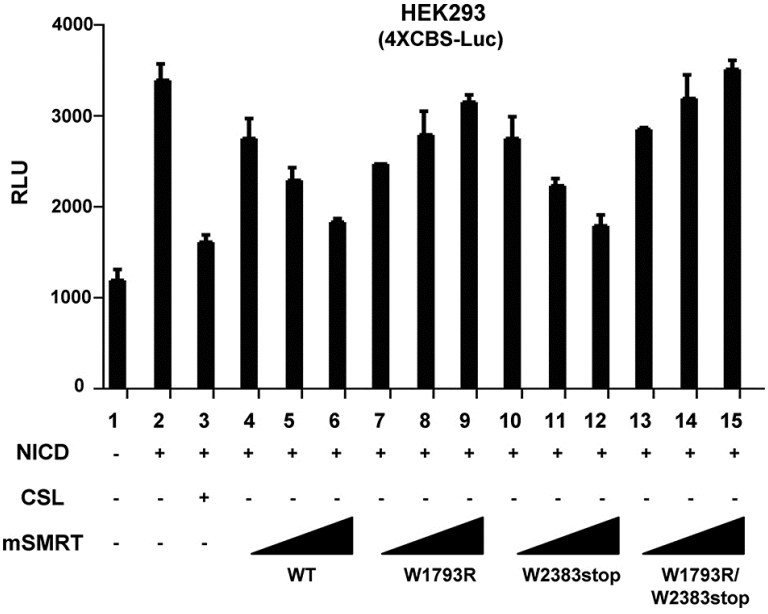

Fig. 7. CSL-interaction motif, rather than SHARP-interaction motif, of SMRT is involved in the transcriptional repression of NICD. HEK293 cells were transfected with 4XCBS-Luc reporter plasmid (100 ng) with or without pCMX-NICD (100 ng), pcDNA3-CSL (50 ng), and indicated pCMX-mSMRT-Flag derivatives (50, 100, and 200 ng). W1793R or W2383stop mutant was constructed to abolish its interaction with CLS or SHARP, respectively. After 48 h of transfection, the cells were harvested, and luciferase activities were measured. The results are the means ±SE values obtained from at least three independent experiments performed in triplicate. WT, wild-type.

was designed not to have C-terminal acidic motif required for interaction with SPOC domain of SHARP.

These constructs were tested for corepressor activity in the NICD-mediated transcription using 4XCBS-Luc reporter gene (Fig. 7). Transient expression of wild-type mSMRT represses transcriptional activity of NICD in a dose-dependent manner to the level of CSL protein did (Fig. 7, lanes 1-6). In contrast to this, CID mutant of mSMRT (W1793R) showed a dominant-negative effect on NICD activity in a dose-dependent fashion (lanes 7-9). Notably, mSMRT mutant (W2382stop) defective in SHARP binding was able to repress the NICD activity as wild-type did (lanes 10-12). As a control, mSMRT mutant containing both mutations showed a dominant-negative pattern, which is similar to that of W1793R mutant (lanes 13-15). This finding suggests the plausible mechanism that SMRT can participate in CSL-mediated repression via its direct binding to CSL without the aid of a bridging factor such as SHARP.

Note: Supplementary information is available on the Molecules and Cells website (www.molcells.org).

ACKNOWLEDGEMENTS

This research was supported by Basic Science Research Programs through the National Research Foundation of Korea (NRF-2014R1A4A1003642 and NRF-2017R1D1A1B03034080) to Y.C.L.

REFERENCES

Ann, E.J., Kim, H.Y., Seo, M.S., Mo, J.S., Kim, M.Y., Yoon, J.H., Ahn, J.S., and Park, H.S. (2012). Wnt5a controls Notch1 signaling through CaMKII-mediated degradation of the SMRT corepressor protein. J. Biol. Chem. *287*, 36814-36829.

Ariyoshi, M., and Schwabe, J.W. (2003). A conserved structural motif reveals the essential transcriptional repression function of Spen proteins and their role in developmental signaling. Genes Dev. *17*, 1909-1920.

Borggrefe, T., and Oswald, F. (2009). The Notch signaling pathway: transcriptional regulation at Notch target genes. Cell. Mol. Life Sci. *66*, 1631-1646.

Borggrefe, T., and Oswald, F. (2014). Keeping notch target genes off: a CSL corepressor caught in the act. Structure *22*, 3-5.

Borggrefe, T., and Oswald, F. (2016). Setting the stage for notch: The Drosophila Su(H)-hairless repressor complex. PLoS Biol. *14*, e1002524.

Chen, J.D., and Evans, R.M. (1995). A transcriptional co-repressor that interacts with nuclear hormone receptors. Nature *377*, 454-457.

Collins, K.J., Yuan, Z., and Kovall, R.A. (2014). Structure and function of the CSL-KyoT2 corepressor complex: a negative regulator of Notch signaling. Structure *22*, 70-81.

Hsieh, J.J., Zhou, S., Chen, L., Young, D.B., and Hayward, S.D. (1999). CIR, a corepressor linking the DNA binding factor CBF1 to the histone deacetylase complex. Proc. Natl. Acad. Sci. USA *96*, 23-28.

Huang, E.Y., Zhang, J., Miska, E.A., Guenther, M.G., Kouzarides, T., and Lazar, M.A. (2000). Nuclear receptor corepressors partner with class II histone deacetylases in a Sin3-independent repression pathway. Genes Dev. *14*, 45-54.

Johnson, S.E., Ilagan, M.X., Kopan, R., and Barrick, D. (2010). Thermodynamic analysis of the CSL x Notch interaction: distribution of binding energy of the Notch RAM region to the CSL beta-trefoil domain and the mode of competition with the viral transactivator EBNA2. J. Biol. Chem. *285*, 6681-6692.

Kao, H.Y., Ordentlich, P., Koyano-Nakagawa, N., Tang, Z., Downes, M., Kintner, C.R., Evans, R.M., and Kadesch, T. (1998). A histone deacetylase corepressor complex regulates the Notch signal transduction pathway. Genes Dev. *12*, 2269-2277.

Kim, J.Y., Park, O.G., Lee, J.W., and Lee, Y.C. (2007). One- plus two-hybrid system, a novel yeast genetic selection for specific missense mutations disrupting protein/protein interactions. Mol. Cell. Proteomics *6*, 1727-1740.

Kim, J.Y., Park, O.G., and Lee, Y.C. (2012). One- plus two-hybrid system for the efficient selection of missense mutant alleles defective in protein-protein interactions. Methods Mol. Biol. *812*, 209-223.

Kopan, R., and Ilagan, M.X. (2009). The canonical Notch signaling pathway: unfolding the activation mechanism. Cell *137*, 216-233.

Kovall, R.A., and Blacklow, S.C. (2010). Mechanistic insights into Notch receptor signaling from structural and biochemical studies. Curr. Topics Dev. Biol. *92*, 31-71.

Kovall, R.A., and Hendrickson, W.A. (2004). Crystal structure of the nuclear effector of Notch signaling, CSL, bound to DNA. EMBO J. *23*, 3441-3451.

Kumar, A., Huh, T.L., Choe, J., and Rhee, M. (2017). Rnf152 is essential for NeuroD expression and Delta-notch signaling in the zebrafish embryos. Mol. Cells *40*, 945-953.

Mikami, S., Kanaba, T., Takizawa, N., Kobayashi, A., Maesaki, R., Fujiwara, T., Ito, Y., and Mishima, M. (2014). Structural insights into the recruitment of SMRT by the corepressor SHARP under phosphorylative regulation. Structure *22*, 35-46.

Mottis, A., Mouchiroud, L., and Auwerx, J. (2013). Emerging roles of the corepressors NCoR1 and SMRT in homeostasis. Genes Dev. *27*, 819-835.

Nam, Y., Sliz, P., Song, L., Aster, J.C., and Blacklow, S.C. (2006). Structural basis for cooperativity in recruitment of MAML coactivators to Notch transcription complexes. Cell *124*, 973-983.

Oberoi, J., Fairall, L., Watson, P.J., Yang, J.C., Czimmerer, Z., Kampmann, T., Goult, B.T., Greenwood, J.A., Gooch, J.T., Kallenberger, B.C., et al. (2011). Structural basis for the assembly of the SMRT/NCoR core transcriptional repression machinery. Nat. Struct. Mol. Biol. *18*, 177-184.

Oswald, F., Tauber, B., Dobner, T., Bourteele, S., Kostezka, U., Adler, G., Liptay, S., and Schmid, R.M. (2001). p300 acts as a transcriptional coactivator for mammalian Notch-1. Mol. Cell. Biol. *21*, 7761-7774.

Oswald, F., Kostezka, U., Astrahantseff, K., Bourteele, S., Dillinger, K., Zechner, U., Ludwig, L., Wilda, M., Hameister, H., Knochel, W., et al. (2002). SHARP is a novel component of the Notch/RBP-Jkappa signalling pathway. EMBO J. *21*, 5417-5426.

Pajerowski, A.G., Nguyen, C., Aghajanian, H., Shapiro, M.J., and Shapiro, V.S. (2009). NKAP is a transcriptional repressor of notch signaling and is required for T cell development. Immunity *30*, 696-707.

Tabaja, N., Yuan, Z., Oswald, F., and Kovall, R.A. (2017). Structure-function analysis of RBP-J-interacting and tubulin-associated (RITA) reveals regions critical for repression of Notch target genes. J. Biol. Chem. *292*, 10549-10563.

VanderWielen, B.D., Yuan, Z., Friedmann, D.R., and Kovall, R.A. (2011). Transcriptional repression in the Notch pathway: thermodynamic characterization of CSL-MINT (Msx2-interacting nuclear target protein) complexes. J. Biol. Chem. *286*, 14892-14902.

Wacker, S.A., Alvarado, C., von Wichert, G., Knippschild, U.,

Wiedenmann, J., Clauss, K., Nienhaus, G.U., Hameister, H., Baumann, B., Borggrefe, T., et al. (2011). RITA, a novel modulator of Notch signalling, acts via nuclear export of RBP-J. EMBO J. *30*, 43-56.

Wilson, J.J., and Kovall, R.A. (2006). Crystal structure of the CSL-Notch-Mastermind ternary complex bound to DNA. Cell *124*, 985-996.

Yuan, Z., Praxenthaler, H., Tabaja, N., Torella, R., Preiss, A., Maier, D., and Kovall, R.A. (2016). Structure and function of the Su(H)-Hairless repressor complex, the major antagonist of notch signaling in Drosophila melanogaster. PLoS Biol. *14*, e1002509.